Communication

Probing the Bottom of a Folding Funnel Using Conformationally Gated Electron Transfer Reactions

Swati Bandi, and Bruce E. Bowler

J. Am. Chem. Soc., **2008**, 130 (24), 7540-7541 • DOI: 10.1021/ja801941r • Publication Date (Web): 22 May 2008

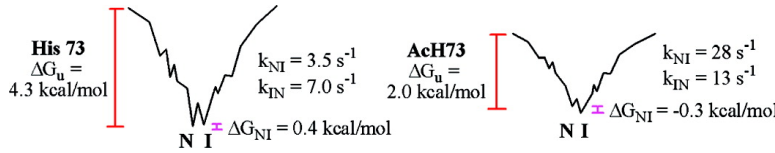

More About This Article

Additional resources and features associated with this article are available within the HTML version:

- Supporting Information
- Access to high resolution figures
- Links to articles and content related to this article
- Copyright permission to reproduce figures and/or text from this article

View the Full Text HTML

J|A|C|S
COMMUNICATIONS

Published on Web 05/22/2008

Probing the Bottom of a Folding Funnel Using Conformationally Gated Electron Transfer Reactions

Swati Bandi and Bruce E. Bowler*

Department of Chemistry and Center for Biomolecular Structure and Dynamics, The University of Montana, Missoula, Montana 59812

Received March 15, 2008; E-mail: bruce.bowler@umontana.edu

The folding funnel concept[1] has provided a useful and effective means of interpreting and understanding the process of protein folding. A key aspect of this model is that foldable proteins favor contacts that lock in the correct topology and thus commit a protein to folding before the protein becomes so compact that the rate of conformational rearrangement becomes slow or glassy. Such minimally frustrated energy landscapes lead to efficient folding, the rate of which increases as the stability of a protein increases.[2] Due to the funneling of the energy landscapes of foldable proteins, less is known about the rate of conformational rearrangements at the bottom of a folding funnel.[2b] While it is clear that decreased protein stability slows the overall rate of protein folding, experimental measurements of the effect of decreased stability on the glassy kinetics at the bottom of a funneled protein folding landscape are lacking. Here, we use engineered proteins in conjunction with novel conformationally gated electron transfer (ET) methods to assess the response of the kinetics at the bottom of a folding funnel to global stability.

In previous work, we have shown that a Lys73→His (K73H) variant of iso-1-cytochrome *c* (iso-1-cyt*c*) stabilizes a compact, partially unfolded form of the protein via His73−heme ligation that is 0.38 ± 0.01 kcal/mol less stable than the native state at pH 7.5.[3] Thermodynamic data are consistent with the red surface loop in Figure 1 being involved in partial unfolding of the protein.[3,4] The global stability of this variant is 4.32 ± 0.12 kcal/mol.[3a] For decreased global stability, we use another variant of iso-1-cyt*c*, AcH73,[5] that also contains the K73H mutation (also contains the mutations T(−5)S and K(−2)L, which lead to N-terminal acetylation, and H33N and H39Q, which remove solvent-exposed histidines; see Supporting Information for details). We confirm here that the global stability of this variant is half-that of the K73H variant (Figure 2; $\Delta G^{\circ}_{u}(H_2O) = 2.02 \pm 0.15$ kcal/mol, $m = 2.68 \pm 0.21$ kcal/(mol × M)).[5] We attribute the loss in global stability to the His26→Asn mutation in this variant, which likely disrupts the bridging hydrogen bond between the green and gray surface loops (Figure 1).[6] To evaluate partial unfolding of the AcH73 variant, guanidine hydrochloride (gdnHCl) denaturation is monitored at 695 nm (loss of the Met80−heme ligation of the native state[7]). At pH 7.5, very little Met80−heme ligation remains even in 0 M gdnHCl. Only at pH 5 (disfavors His73−heme ligation) is substantial Met80−heme ligation seen at 0 M gdnHCl (Figure 2). The native Met80−heme (N) to His73−heme partially unfolded form (I) equilibrium of the AcH73 variant is measured by pH titration observed at 695 nm (Figure 2, inset), yielding $\Delta G_{NI} = -0.3 \pm 0.2$ kcal/mol. Thus, the global stability of the AcH73 variant is 2-fold lower than that of the K73H variant, and the relative stabilities of the N and I forms are similar, although for the AcH73 variant I is more stable than N at pH 7.5.

The pH dependence of the N to I equilibrium allows the kinetics of interconversion between these states to be monitored by pH jump

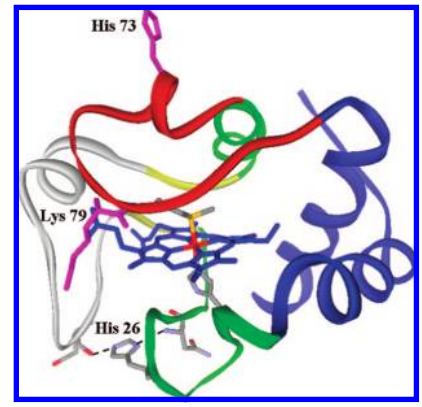

Figure 1. Iso-1-cyt*c* showing the side chains of His73 (K73H mutation) and Lys79 as stick models. The heme cofactor is shown in blue with the heme ligands Met80 and His18 colored by atom type. The side chain of His26 is shown hydrogen-bonded to the carbonyl of Glu44 and the amide NH of Asn31. The substructures of cytochrome *c* as defined by Englander and co-workers[4] are shown from least to most stable in the colors gray, red, yellow, green, and blue.

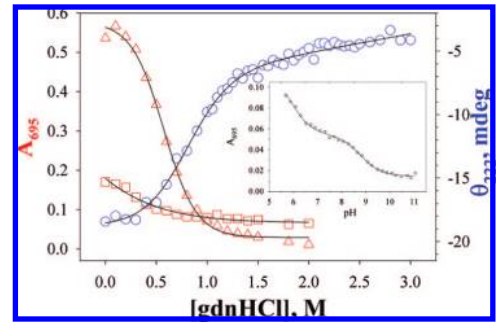

Figure 2. Global (open blue circles, pH 7.5) and partial unfolding (open red squares, pH 7.5, open red triangles, pH 5.0) of the AcH73 variant due to gdnHCl at 25 °C monitored by circular dichroism and at 695 nm, respectively. Solid curves are fits of the data to a two-state model. Inset: pH-dependent partial unfolding of the AcH73 variant monitored at 695 nm. Solid curve is a fit to a model[3b] involving partial unfolding to a His73−heme form near pH 7.5 and a Lys79−heme form at higher pH.

stopped-flow mixing, yielding $k_{obs} = k_{NI} + k_{IN}$. Near physiological pH, k_{obs} varies little with pH for the AcH73 variant and is about 3-fold the magnitude of k_{obs} for the K73H variant[8] (Figure 3). Due to the complex pH dependence of the N to I kinetics,[8] k_{NI} and k_{IN}, needed to assess the relative height of the barrier between N and I, in the stable K73H versus the unstable AcH73 variant, are difficult to extract from k_{obs} near pH 7.

We take advantage of a novel gated ET method, which allows trapping of the native conformer as it forms[9] to evaluate k_{NI} and k_{IN} for the AcH73 variant. The low reduction potential of I (∼0

10.1021/ja801941r CCC: $40.75

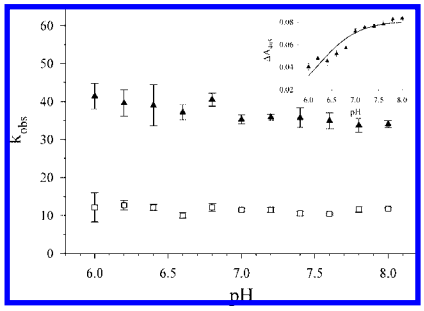

Figure 3. Observed rate constant, k_{obs} (s^{-1}), as a function of pH at 25 °C for the formation of the partially unfolded form of the AcH73 (filled triangles) and K73H (open squares, data from ref 8) variants. Initial conditions were pH 5, 0.1 M NaCl, and final conditions were 0.1 M NaCl and 10 mM buffer at the indicated pH after stopped flow mixing. Inset shows amplitude data for the AcH73 variant.The solid curve is a fit of the data to a conformational transition triggered by one ionizable group. The fit yields $pK_H = 6.7 \pm 0.1$, consistent with ionization of His73.

Scheme 1. Gated ET Kinetic Mechanism

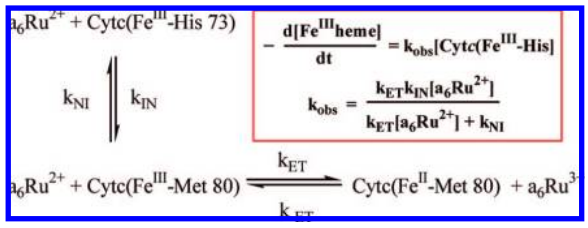

mV vs NHE) relative to N (290 mV vs NHE) leads to selective reaction of the inorganic reagent, hexaammineruthenium(II) chloride (a_6Ru^{2+}) with N (Scheme 1).[9] When $k_{ET}[a_6Ru^{2+}] \gg k_{NI}$, k_{obs} for reduction of the His73−heme conformer is equal to k_{IN} (gated ET), and when $k_{NI} \gg k_{ET}[a_6Ru^{2+}]$, $k_{obs} \approx k_{ET} \times K_{IN}$ (coupled ET). At pH 7.5, the I to N ratio is about 2:1 for the AcH73 variant. Thus, reaction with a_6Ru^{2+} yields a fast phase due to direct ET with N and a slower phase due to ET starting from I (Supporting Information). For each phase, k_{obs} as a function of $[a_6Ru^{2+}]$ is shown in Figure 4. Clearly, the ET reaction of I proceeds from the coupled to the gated ET regimes.[10] Using $k_{ET} = 56 \pm 1$ mM^{-1} s^{-1} (Figure 4, inset), a fit of the ET data for I to the expression for k_{obs} in Scheme 1 yields $k_{NI} = 28.1 \pm 2.4$ s^{-1} and $k_{IN} = 13.1 \pm 0.2$ s^{-1}.

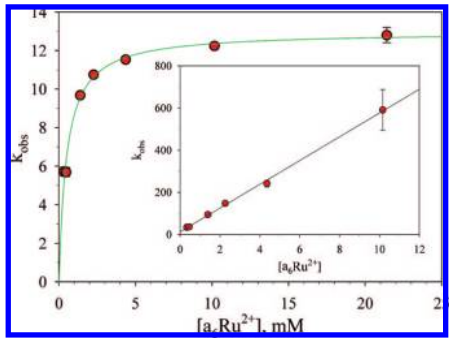

Figure 4. Observed pseudo-first-order rate constant, k_{obs} (s^{-1}), for the reaction of a_6Ru^{2+} with the His73−heme conformer of the AcH73 variant as a function of $[a_6Ru^{2+}]$. The solid curve is a fit of the data to the equation in Scheme 1. Data were acquired at 25 °C in the presence of 10 mM sodium phosphate pH 7.5, 0.1 M NaCl. Inset shows k_{obs} (s^{-1}) for the reaction of a_6Ru^{2+} with the native conformer of the AcH73 variant as a function of $[a_6Ru^{2+}]$. A straight line fit yields $k_{ET} = 56 \pm 1$ mM^{-1} s^{-1}.

At pH 7.5, $k_{NI} = 3.5 \pm 0.2$ s^{-1} and $k_{IN} = 7.0 \pm 0.4$ s^{-1} for the more stable K73H variant. Thus, the kinetics of the interconversion of N and I for the less stable AcH73 variant are faster in both directions, consistent with the barriers at the bottom of a folding funnel decreasing as a protein becomes less stable.

The global folding kinetics of cyt*c* at high driving force in the absence of misfolding are fast ($\tau \sim 10$ ms),[11] compared to the conversion of I to N at pH 7.5 for either the K73H or the AcH73 variant ($\tau \sim 100$ ms). Thus, the rate of formation of N from the compact I state is slow as expected for glassy behavior. Multiexponential kinetics is not observed, indicating that I and N dominate the bottom of the energy landscape of these proteins.

For random sequence proteins, energy landscape theory predicts a flattened landscape with sizable barriers between minima in the energy landscape.[1b] Our data indicate that the funneled landscapes of foldable proteins behave very differently when they flatten out. In a funneled landscape, lower stability seems to relax barriers between conformations. This observation is analogous to the behavior of cold-adapted enzymes from psychrophilic organisms. The dynamics in these less stable enzymes are enhanced, allowing the catalytically active state to still be readily accessed at low temperature.[12] Thus, it appears that funneled landscapes have evolved such that even unstable proteins are unlikely to become trapped in alternate conformers en route to the native state.[13]

Acknowledgment. The authors acknowledge support of this research by NSF Grant CHE-0650156 (B.E.B.).

Supporting Information Available: Experimental methods for gdnHCl denaturation, pH titrations, pH jump stopped-flow and gated ET measurements. Figures showing typical pH jump stopped flow and gated ET data and tables of rate constants. This material is available free of charge via the Internet at http://pubs.acs.org.

References

(1) (a) Bryngelson, J. D.; Onuchic, J. N.; Socci, N. D.; Wolynes, P. G. *Proteins* **1995**, *21*, 167–195. (b) Wolynes, P. G. *Philos. Trans. R. Soc. A* **2005**, *363*, 453–467.
(2) (a) Mines, G. A.; Pascher, T.; Lee, S. C.; Winkler, J. R.; Gray, H. B. *Chem. Biol.* **1996**, *3*, 491–497. (b) Oliveberg, M.; Wolynes, P. G. *Q. Rev. Biophys.* **2005**, *38*, 245–288.
(3) (a) Godbole, S.; Dong, A.; Garbin, K.; Bowler, B. E. *Biochemistry* **1997**, *36*, 119–126. (b) Nelson, C. J.; Bowler, B. E. *Biochemistry* **2000**, *39*, 13584–13594. (c) Nelson, C. J.; LaConte, M. J.; Bowler, B. E. *J. Am. Chem. Soc.* **2001**, *123*, 7453–7454.
(4) (a) Bai, Y.; Sosnick, T. R.; Mayne, L.; Englander, S. W. *Science* **1995**, *269*, 192–197. (b) Krishna, M. M. G.; Lin, Y.; Rumbley, J. N.; Englander, S. W. *J. Mol. Biol.* **2003**, *331*, 29–36.
(5) Hammack, B. N.; Smith, C. R.; Bowler, B. E. *J. Mol. Biol.* **2001**, *311*, 1091–1104.
(6) Wandschneider, E.; Hammack, B. N.; Bowler, B. E. *Biochemistry* **2003**, *42*, 10659–10666.
(7) Moore, G. R., and Pettigrew, G. *Cytochrome c: Evolutionary, Structural and Physicochemical Aspects*; Springer-Verlag: New York, 1990; pp 69−70.
(8) Martinez, R. E.; Bowler, B. E. *J. Am. Chem. Soc.* **2004**, *126*, 6751–6758.
(9) (a) Baddam, S.; Bowler, B. E. *J. Am. Chem. Soc.* **2005**, *127*, 9702–9703. (b) Baddam, S.; Bowler, B. E. *Inorg. Chem.* **2006**, *45*, 6338–6346. ET methods have also been used to initiate protein folding; see ref 2a for example.
(10) Progression from coupled to gated ET has been observed for inorganic complexes: Wijetunge, P.; Kulatilleke, C. P.; Dressel, L. T.; Heeg, M. J.; Ochrymowycz, L. A.; Rorabacher, D. B. *Inorg. Chem.* **2000**, *39*, 2897–2905.
(11) (a) Hammack, B. N.; Godbole, S.; Bowler, B. E. *J. Mol. Biol.* **1998**, *275*, 719–724. (b) Rumbley, J. N.; Hoang, L.; Englander, S. W. *Biochemistry* **2002**, *41*, 13894–13901.
(12) D'Aminco, S.; Marx, J.-C.; Gerday, C.; Feller, G. *J. Biol. Chem.* **2003**, *278*, 7891–7896.
(13) Lattman, E. E.; Rose, G. D. *Proc. Natl. Acad. Sci. U.S.A.* **1993**, *90*, 439–441.

JA801941R